ORIGINAL ARTICLE

AG-2018-122
dx.doi.org/10.1590/S0004-2803.201900000-02

# $^{18}$F-FDG PET/CT as an assessment tool of hepatocellular carcinoma secondary to non-alcoholic fatty liver disease development in experimental model

Caio de Souza **LEVY**, Fernando Gomes de Barros **COSTA**, Daniele de Paula **FARIA**, Jose Tadeu **STEFANO**, Bruno **COGLIATI** and Claudia P **OLIVEIRA**

Received 12/10/2018
Accepted 23/1/2019

**ABSTRACT** – **Background** – Hepatocellular carcinoma (HCC) can be the last step of non-alcoholic fatty liver disease (NAFLD) evolution. Experimental models are crucial to elucidate the pathogenesis of HCC secondary to NAFLD. The 2-deoxy-2-($^{18}$F)fluoro-D-glucose ($^{18}$F-FDG) positron emission tomography/computed tomography (PET/CT) plays an important role in evaluating HCC development and progression. **Objective** – To standardize the imaging method of PET/CT with $^{18}$F-FDG as an evaluation tool of the experimental model of HCC secondary to NAFLD. **Methods** – Ten male Sprague-Dawley rats were fed with choline-deficient high-fat diet and diethylnitrosamine (DEN) in the drinking water for 16 weeks and then received 1 mL of saline solution (0.9%) daily by gavage for three weeks. At the 16th and 19th weeks, abdominal ultrasonography (USG) was performed. $^{18}$F-FDG PET/CT images were obtained before the beginning of experiment (week 0) and at the end (week 19). Histological and immunohistochemically analysis were also performed. **Results** – The USG results showed a homogeneous group at the 16th week with an average of 4.6±2.74 nodules per animal. At the 19th week, PET/CT findings demonstrated an average of 8.5±3.7 nodules per animal. The mean values of SUVmed and SUVmax were 2.186±0.1698 and 3.8±1.74, respectively. The average number of nodules per animal in the histological analysis was 5.5±1.5. From all nodules, 4.6% were classified as well-differentiated HCC and 81.8% were classified as poorly-differentiated HCC. **Conclusion** – $^{18}$F-FDG PET/CT was able to evaluate the development of HCC in an experimental model of NAFLD non-invasively. From the standardization of PET/CT in this model, it is possible to use this tool in future studies to monitor, *in vivo* and non-invasively, the progression of HCC.

**HEADINGS** – Hepatocellular carcinoma. Non-alcoholic fatty liver disease. Positron emission tomography computed tomography. Fluorodeoxyglucose F18. Animal models.

## INTRODUCTION

The non-alcoholic fatty liver disease (NAFLD) has been considered the hepatic manifestation of metabolic syndrome and has an increasing prevalence around the world[1,2]. It includes a broad spectrum of disease since simply steatosis, non-alcoholic steatohepatitis (NASH) and hepatocellular carcinoma (HCC), being able to progress directly from steatosis to HCC[3].

Liver cancer is the second cause of death related to cancer worldwide, with HCC being the most common liver cancer[4]. The risk of dying from liver cancer is 4.5 times higher in obese men when compared to men with normal body mass index (BMI), corroborating with the idea that the high incidence of HCC is associated to the increase of NAFLD cases, specifically NASH, which is highly linked to the global burden of obesity and type 2 diabetes[5].

The development of experimental models is of extreme importance to elucidate de pathogenesis of HCC secondary to NAFLD and to analyze the interference of drugs in the natural disease course. These models must be able to simulate the HCC genesis in humans, including hypercaloric diet, obesity, insulin resistance (IR), same natural disease course, similar genetic aspects and activation of same signaling pathways[6,7]. Several models were developed with this purpose despite none of these models is widely accepted yet[8,9].

Experimental induction of HCC can be analyzed by diverse imaging modalities as contrast enhanced ultrasonography (CEUS), computed tomography (CT) and magnetic resonance imaging (MRI). Recently, our group demonstrated a good accuracy of CEUS and elastography for the diagnosis of well and moderately-differentiated HCC in experimental model of NASH induced by choline-deficient high-fat diet and diethylnitrosamine (DEN)[10]. In this context, positron emission tomography (PET) with 2-deoxy-2-($^{18}$F)fluoro-D-glucose ($^{18}$F-FDG) associated to CT has been shown to be useful to detect HCC, evaluate tumor progression and investigate metastasis[11-13]. However, there is still a lack of studies to evaluate the progression of HCC secondary to NAFLD with $^{18}$F-FDG PET/CT. The aim of this study is to standardize the $^{18}$F-FDG PET/CT as an evaluation tool of the experimental model of HCC secondary to NAFLD.

Declared conflict of interest of all authors: none
Disclosure of funding: no funding received
Universidade de São Paulo, Faculdade de Medicina, Departamento de Gastroenterologia (LIM-07) e Laboratório de Medicina Nuclear (LIM-43), Departamento de Radiologia e Oncologia. Universidade de São Paulo, Faculdade de Medicina Veterinária e Zootecnia, Departamento de Patologia. São Paulo, SP, Brasil.
Corresponding author: Claudia P Oliveira. E-mail: cpm@usp.br; claudia.oliveira220@fm.usp.br.

## METHODS

Ten 3-month-old male Sprague-Dawley rats, weighting 300-400 g, were housed in the animal facility of the Clinical and Experimental Gastroenterology Laboratory (LIM-07) of the University of São Paulo Medical School (FMUSP). The animals were kept in a room with ventilation, relative humidity, controlled temperature and light/dark cycle 12:12, and were given water ad libitum. The study was approved by the ethics committee in animal use of USP Medical School (nº 108/14) and all animals received humane care according to the criteria outlined in the "Guide for the Care and Use of Laboratory Animals".

For the HCC secondary to NAFLD development, the animals were fed with choline-deficient high-fat diet [35% of total fat, enriched with 54% of fatty acids (Rhoster Ltda, Brazil)] and DEN dose of 100 mg/L in the drinking water ad libitum for 16 weeks, according to our previous study[14]. After this period, the carcinogenic stimulus was removed and the rats received 1 mL of saline solution (0.9%) daily by gavage for three weeks.

At the 16th and 19th weeks of experimentation, abdominal ultrasonography (USG) was performed for quantification, measurement and location of hepatic nodules. The exam was performed using the Phillips Ultrasound IU 22 (Bothell, WA, USA) equipment with VL13-5 transductor. Before the procedure, the animals were anesthetized intraperitoneally with ketamine (Cristalia, Brazil) dose of 80 mg/kg and xylazine (Bayer, Brazil) dose of 10 mg/kg. Nodules ≥0.2 cm were considered.

For PET/CT, the PET/CT/SPECT equipment for small animals, model Triumph Trimodality, was used (Gamma Medical-Ideas, Northridge, CA, USA), illustrated in FIGURE 1. The [18]F-FDG PET/CT images were obtained before the beginning of experiment (Baseline – week 0) and at the end (week 19). Before the procedure, animals were anesthetized with isoflurane 5% with oxygen 100% for induction and isoflurane 2%-3% with oxygen 100% for maintenance.

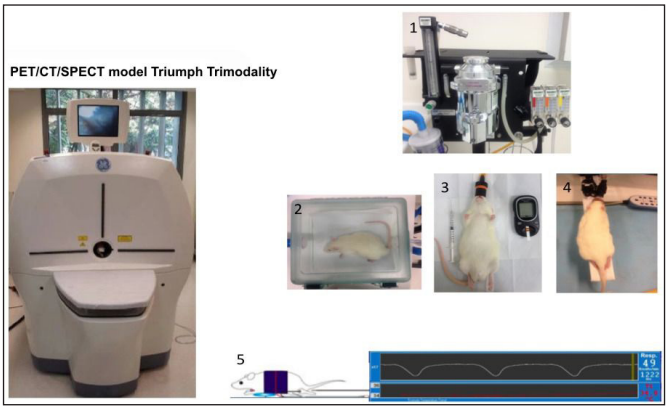


**FIGURE 1.** Photo of PET/CT equipment. 1 – inhalation anesthesia equipment, 2 – box for inhalation anesthesia induction, 3 – anesthetized rat, syringe with 18F-FDG and glucometer, 4 – anesthetized and positioned rat in PET, 5 – illustration of rat monitoring.

After being anesthetized, the animals were weighed and had their blood glucose level tested. The average of [18]F-FDG injected, by the penile vein, on each animal was 37.7±6.29 MBq (1.02±0.17 mCi). The PET images were obtained for 30 minutes, 45 minutes after the [18]F-FDG injection and reconstructed by the interactive method OSEM-3D, 20 interactions and 4 subsets with transversal vision field of 100 mm, matrix of 240 x 240 and pixel of 0.42 x 0.42 mm. The CT imagens were obtained with 65 kVp, 165 mA in 512 projections and magnification of 1.3 for anatomic correlation, being reconstructed with the Filtered Back-projection (FBP) method, matrix of 512 x 512 and pixel of 0.17 x 0.17 mm. Both images were exported with DICOM format and analyzed by PMOD® software (PMOD Technologies Ltd., Zurich).

The tumor regions of interest (ROI) were drawn and the values were expressed in standardized uptake value (SUV), being calculated the SUVmed and SUVmax. After the procedure, animals were kept in micro-isolators for 10 half-lives of the radioisotope (18 hours). three days after PET/CT, the animals were euthanized with intraperitoneally injection of ketamine, dose of 120 mg/kg, followed by exsanguination.

For histological analysis, hepatic tissue samples were fixed in 10% phosphate-buffered formalin for 24 hours and embedded in paraffin wax. Samples were cut into 5 µm sections and stained with hematoxylin-eosin for evaluation of steatosis, hepatocellular ballooning, lobular inflammation and NAFLD activity score (NAS) as previously described[15]. The HCC classification was done according to the characteristics defined by Thoolen et al.[16], specifically for rats, and graded according to Edmondson & Steiner's classification[17].

For immunohistochemistry analysis, formalin-fixed paraffin-embedded tissues were sectioned at 5 µm. The heat-induced epitope retrieval was performed in an electric pressure coocker (110V, 60Hz) for 15 mins, using citrate (pH 6.0) buffer. After blocking endogenous peroxidase with 6% $H_2O_2$ solution (Merck, USA) for 30 min, the slides were incubated in a humidified chamber overnight at 4°C with the rabbit primary anti-HepPar1 (Dako, 1:500), cytokeratin 19 (CK19, Leica Novocastra, 1:200) e glutamine-synthetase (GS, Millipore, 1:3000). Slides were then incubated with the complex Super Picture Polymer Detection kit (Life Technologies, USA) for 30 min at 37°C. After incubation, the reaction was visualized with 3'3 diaminobenzidine chromogen and the slides were slight counterstain with Harris hematoxylin. Negative controls were performed replacing the primary antibody with homologous non-immune sera. Nodules immunostained with HepPar1 and GS, and negative with CK19 were considered HCC.

For statistical analysis, values of mean, median and standard deviation were calculated according to the distribution pattern of variables using the software GraphPad Prism version 7.

## RESULTS

Nine animals completed the 16 weeks of experimentation. The mean overall survival along the experiment was 126.3±8.5 days, with median of 130 days. The main causes of death were pneumonia, hemorrhagic ascites, tumor rupture and respiratory insufficiency during anesthetic induction for PET/CT. The average weight was maximum at the 16th week (479.5±45.4 g), decreasing after this period to an average of 440.5±67 g per animal at the 19th week.

The USG results showed a homogeneous group at the 16th week with average of 4.6±2.74 nodules per animal. At the 19th week, only four rats remaining were submitted to the second USG, which demonstrated a high increase of nodules per animal. The majority of these nodules were disposed at the left lobe, as shown in TABLE 1.

**TABLE 1.** Ultrasonography findings.

| Week of abdominal USG | 16th week | 19th week |
|---|---|---|
| Number of nodules >0.2 cm | 42 | 39 |
| Biggest nodule (cm) | 2.6 | 3.8 |
| Mean of nodules per animal | 4.6±2.74 | 9.75±0.96 |
| Median of nodules | 4 | 9.5 |
| Nodules on left lobe | 61.9% | 48.7% |
| Nodules on right lobe/caudate lobe | 21.4% | 46.2% |
| Nodules on medium lobe | 16.7% | 5.1% |
| Ascites | 11.1% | 100% |

USG: ultrasonography.

At the beginning of experimentation, the [18]F-FDG PET/CT was standardized and the ROI were drawn at the right, medium and left lobes of liver, revealing the absence of hepatic lesions in all rats. After 19 weeks, the four alive rats were submitted to [18]F-FDG PET/CT again, which demonstrated an average of 8.5±3.7 nodules per animal, as illustrated in FIGURE 2. It was verified only 2 hyper-uptake lesions with hypo-uptake center and 32 homogeneous hyper-uptake lesions. The mean values of SUVmed and SUVmax were 2.186±0.1698 and 3.8±1.74, respectively.

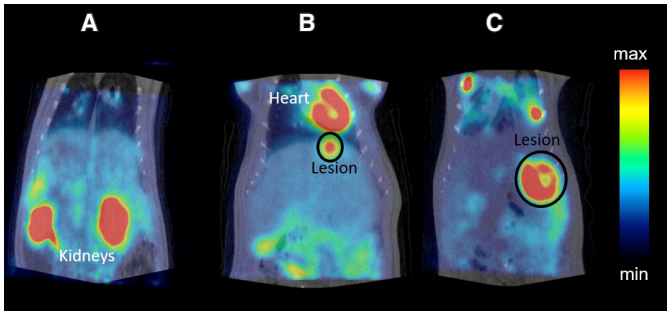


**FIGURE 2.** Illustrative 18F-FDG PET/CT fused images (coronal view). A) Baseline scan, where no liver lesion was observed; B) 19 weeks scan showing homogeneous hyper-uptake lesion in liver (black circle) and C) 19 weeks scan showing a hyper-uptake lesion with hypo-uptake center (black circle).

The average number of nodules per animal in the histological analysis was 5.5±1.5. All the samples showed histological hepatic steatosis, with stage 4 fibrosis and NAS of 4. From all nodules, 4.6% were classified as well-differentiated HCC (Grades I/II of Edmondson & Steiner's classification) and 81.8% were classified as poorly-differentiated HCC (Grades III/IV of Edmondson & Steiner's classification) (FIGURE 3). Other histological findings are shown in TABLE 2.

## DISCUSSION

Non-invasive methods to evaluate hepatic tumors are able to reduce the necessary number of animals to provide statistically significant results, facilitating the execution of studies to assess tumor development, progression and monitor the therapeutic response to a new modality of treatment. In this context, the present study attempted to apply the PET/CT with [18]F-FDG as an evaluation tool of the HCC secondary to NASH in an experimental model of NAFLD.

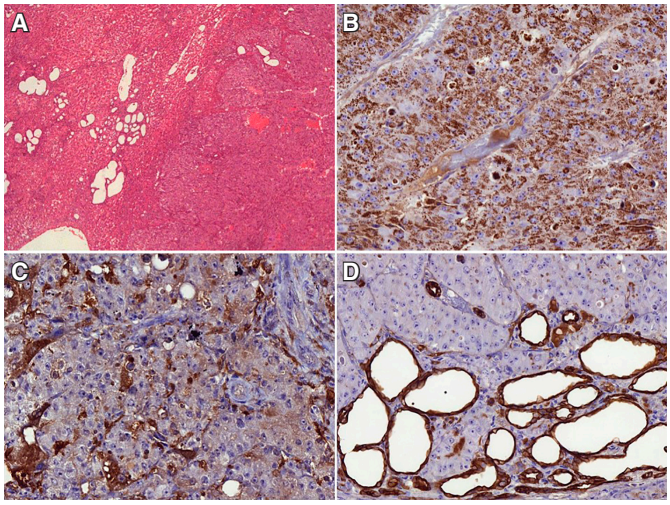


**FIGURE 3.** Representative photomicrographs of histological and immunohistochemical analysis of hepatocellular carcinoma related to NAFLD in rats. HE staining (A) (50×). Positive immunostaining of HepPar-1 (B) and glutamine-synthetase (C) in the neoplastic cells. D) Negative immunostaining of cytokeratin 19 in the neoplastic cells, but positive immunoexpression in the biliary cysts. Immunohistochemistry with Harris' hematoxylin counterstain (400x).

**TABLE 2.** Histological findings.

| | |
|---|---|
| Number of analyzed nodules | 22 |
| Mean of nodules per animal | 5.5±1.5 |
| Dysplastic nodules | 13.6% |
| Grade I/II HCC nodules | 4.6% |
| Grade III/IV HCC nodules | 81.8% |
| Nodules with vascular invasion | 13.6% |
| Hemorrhagic nodules | 31.8% |
| Nodules with necrosis | 40.9% |
| Biliary cysts | 18.2% |

HCC: hepatocellular carcinoma.

Some studies were able to demonstrate the applicability of non-invasive methods in HCC experimental models before. One of these studies, used PET to evaluate HCC model of orthotropic implantation of tumor cells by injection[18]. However, it is known that DEN induced HCC is able to provide better tumor perfusion, heterogeneity and higher genetic similarity to the human model of HCC than orthotropic implantation[19].

A previous analysis of 7 animal models concluded that the genetic expression patterns of DEN induced HCC were similar to human HCC with poor prognostic[20]. Besides, in our previous study, it was demonstrated that the use of choline-deficient high-fat diet in association to DEN is able to provide NASH and fibrosis, simulating all the steps of HCC development in NAFLD context[14]. In front of this, the model of choline deficient high-fat diet associated to DEN was chosen because it was useful in simulating the genetic and environmental factors of HCC development in humans.

Previous studies also evaluated the use of [18]F-FDG PET/CT in experimental models of HCC. In an analysis of rats with HCC by intraperitoneally DEN injection or hepatitis B virus (HBV) trans-

genic X protein expression, the [18]F-FDG PET/CT was shown able to evaluate the tumor development and monitor HCC progression. Besides, it was demonstrated a higher [18]F-FDG uptake in poorly-differentiated tumors compared to well-differentiated tumors, and positive relation between SUVmax values and tumor size[13].

In other study, HCC was developed with weekly intraperitoneal injection of DEN for 16 weeks and evaluated with [18]F-FDG PET/CT. With this method, it was possible to follow the tumor development and its progression during the weeks 14, 16, 18 and 20 of experimentation, showing the [18]F-FDG PET/CT as an useful tool in measuring tumor growth[12].

One of the first studies to assess the application of [18]F-FDG PET/CT used c-Myc transgenic rats associated to the carcinogen N-nitrosodiethylamine (NDEA)[11]. This work showed the utility of [18]F-FDG PET/CT on the quantitative evaluation of HCC, follow-up of tumor growth, metastasis and secondary tumor growth detection. However, although the evaluation of experimental HCC by this imaging method have already been explored in some studies, to our knowledge, the present study is the first to evaluate the development of HCC in an experimental model of NAFLD with [18]F-FDG PET/CT.

By this experimental model, it was possible to observe the development of steatosis and grade 4 hepatic fibrosis in all studied samples, proving the development of NAFLD. Besides, the NAS of all samples was 4, evidencing the presence of NASH. The majority of studied nodules were classified in grade III or IV of Edmondson & Steiner's classification, representing poorly-differentiated tumors, which tend to have worse prognosis and to determinate more advanced disease. This is probably due to the fact of long time of exposition to DEN (16 weeks) and the wait of more three weeks to animals sacrifice and histological analysis, giving more time to tumor progression.

Such great severity of the disease at the 19th week is evidenced also by the presence of ascites in 100% of animals analyzed by abdominal USG comparing to only 11.1% of animals with ascites at the 16th week of experimentation. Besides, at the 16th week only 1 rat has died, meantime with the progression of the disease in three weeks only four rats remained alive to complete the experiment.

In a model of HCC secondary to NASH, induced with high-fat/fructose diet and sedentary lifestyle, it was demonstrated the NASH development at six months of experimentation and the HCC development at 12 months in only 60% of animals[21]. This result shows that is possible to induce HCC experimentally in a model that simulates the majority of NAFLD patient's lifestyle. However, there is a difficulty in the reproducibility of this kind of model because of the longtime of experimentation needed to tumor development. On the other hand, the present study used a model previously described[14], which needs only 16 weeks to obtain HCC and NASH in all animals, what turns more practical the reproducibility of the experiment, monitoring of tumor progression and response evaluation of some therapeutic modality.

Other studies also took a long time to demonstrate the development of HCC and NASH. Two models were developed with C57BL/6J rats, genetically predisposed, after high-fat diet consume. The study DIAMOND used high-fat diet in association to ad libitum consume of glucose and fructose[7], in the meantime the other study used choline-deficient, L-aminoacid-defined, high-fat diet (CDAHFD)[22]. In the DIAMOND model, the HCC was developed in 89% of the studied rats between 32 and 52 weeks of experimentation. In the CDAHFD model, the HCC was verified only in four of the 15 rats analyzed between 36 and 60 weeks of exposition to this diet. In contrast, all rats developed hepatocellular adenoma during the experimentation.

In the present study, 81.8% of analyzed nodules were categorized as poorly-differentiated HCC (Grades III/IV of Edmondson & Steiner's classification), what may have occurred due to the period of experimentation since were waited three weeks, after the 16 weeks of exposure to DEN, to perform [18]F-FDG PET/CT and sacrifice the animals. Moderately or poorly-differentiated tumors have low levels of glucose-6-phospatase enzyme, which participates of glucose metabolism in the hepatocytes, and due to this fact accumulate more [18]F-FDG than well-differentiated tumors, being better visualized with [18]F-FDG PET/CT[23]. It was demonstrated in patients which the performed [18]F-FDG PET was able to obtain a sensitivity of 88% in moderately or poorly-differentiated HCC detection. In contrast, [18]F-FDG PET sensitivity drops to 50% when well-differentiated HCC is analyzed[24]. Therefore, the great viability to detect HCC with [18]F-FDG PET/CT in our study may have been influenced by the histological HCC pattern found.

Though the PET is not recommended as a diagnostic tool in HCC detection, it has already been demonstrated that can be useful to detect metastasis, evaluate treatment response and staging to better therapeutic decision and prognostic[25]. Sugiyama et al. demonstrated that [18]F-FDG PET sensitivity in extra-hepatic detection of HCC metastasis is 83%[26]. This data is in agreement with the sensitivity obtained by Park et al. of 85.7% in detecting metastatic HCC with PET[27]. Yoon et al. also demonstrated that PET/CT has more accuracy in HCC metastasis detection than CT isolated or MRI[28]. In a meta-analysis comparing PET with USG, CT and MRI, the PET was considered de non-invasive method with higher sensitivity to detect hepatic metastasis of colorectal, gastric and esophageal primary tumors[29]. Other meta-analysis of 8 studies concluded that [18]F-FDG PET/CT has a good performance in diagnostic of metastatic HCC and disease recurrence, and can contribute to better management of HCC patients and higher accuracy of staging[30].

The limitation of our study was the absence of 16th week [18]F-FDG PET/CT as we could not follow the evolution of the same node with one diagnostic tool throughout the experiment. However, our mortality rate was high, in terms of exposing the same animal to two PET/CT imaging procedures with inhalational anesthesia, as this can heighten the rate; this is why we chose USG at the 16th week, which showed that the group was homogeneous and the experiment was feasible.

On the other hand, in humans there is evidence that PET is able to detect residual tumor after radiofrequency ablation earlier than CT and MRI, identifying residual disease only 1 week after the procedure[31]. The [18]F-FDG PET has proven to be able to evaluate the response to a neoadjuvant loco-regional treatment, as radiofrequency ablation or transarterial chemoembolization (TACE), and to predict the outcome after this kind of intervention[32-34]. Some studies have also described the applicability of PET in monitoring the response of HCC to sorafenib[35] and demonstrated the [18]F-FDG uptake as an independent prognostic factor in patients treated with this drug[36].

Besides, diverse authors demonstrated the applicability of PET as a prognostic tool in hepatic resection. In a study of HCC patients submitted to hepatic resection, Seo et al. reported that survival rates and free-disease survival were significantly lower in patients with the relation tumor SUV and non-tumor SUV (RTN) >2 before treatment compared to the group of patients that the relation was

<2. In multivariate analysis, high values of RTN and high values of a-fetoprotein were considered independent predictors of tumor recurrence after surgery[37]. In a meta-analysis of 22 studies with 1721 patients, SUV value and RTN before HCC treatment were associated to bad outcome[38], demonstrating the applicability of $^{18}$F-FDG PET in HCC prognosis. In a series of cases of patients submitted to hepatic transplantation, Detry et al. also demonstrated that the relation between tumor SUVmax and non-tumor SUVmax was the only independent prognostic factor able to predict tumor recurrence, stablishing a cut point of 1.15[39]. This fact was confirmed by Lee et al., demonstrating that 97% of HCC patients with tumor SUVmax/non-tumor SUVmax <1.15 before hepatic transplantation did not present tumor recurrence in two years. In contrast, only 42% of patients with the relation above 1.15 did not present tumor recurrence in this period[40]. Finally, using the results of $^{18}$F-FDG PET/CT and the measured tumor size, a new criteria of patient selection for hepatic transplantation with living-donor was recently proposed, named The National Cancer Center Korea (NCCK) Criteria[41], what demonstrates the utility of PET/CT in the management of HCC patients.

## CONCLUSION

The present study was able to evaluate the development of HCC in an experimental model of NAFLD using PET/CT with $^{18}$F-FDG non-invasively correlating the PET/CT findings with USG and confirming the HCC diagnosis through histological and immunohistochemically analysis. These results show the applicability of this imaging modality in HCC secondary to NAFLD experimental studies. From the standardization of PET/CT in this model, it is possible to use this tool in future studies to monitor, in vivo and non-invasively, the progression of HCC.

## ACKNOWLEDGEMENTS

We want to thank *Coordenação de Aperfeiçoamento de Pessoal de Nível Superior* (CAPES) for supporting this survey through the *Programa Institucional de Bolsas de Iniciação Científica* (PIBIC).

### Authors' contribution

Levy CS: data collection, survey execution and writing of text. Costa FGB: data collection and survey execution. Faria DP: data collection and survey execution. Stefano JT: text revision. Cogliati B: survey execution. Oliveira CP: survey execution and text revision.

### Orcid

Caio de Souza Levy. Orcid: 0000-0002-6069-9285.
Fernando Gomes de Barros Costa. Orcid: 0000-0001-8885-3531.
Daniele de Paula Faria. Orcid: 0000-0002-1766-2786.
Jose Tadeu Stefano. Orcid: 0000-0002-0218-1920.
Bruno Cogliati. Orcid: 0000-0002-1388-7240.
Claudia P Oliveira. Orcid: 0000-0002-2848-417X.

Levy CS, Costa FGB, Faria DP, Stefano JT, Cogliati B, Oliveira CP. PET/CT com $^{18}$F-FDG como ferramenta de avaliação do desenvolvimento de carcinoma hepatocelular secundário a doença hepática gordurosa não alcoólica em modelo experimental. Arq Gastroenterol. 2019;56(1):45-50.

**RESUMO** – **Background** – O carcinoma hepatocelular (CHC) pode ser a última fase da doença hepática gordurosa não alcoólica (DHGNA). Modelos experimentais são cruciais para elucidação da patogênese do CHC secundário a DHGNA. A tomografia por emissão de pósitrons/tomografia computadorizada (PET/TC) com 2-desoxi-2-($^{18}$F)fluoro-D-glicose ($^{18}$F-FDG) desempenha um importante papel na avaliação do desenvolvimento e progressão do CHC. **Objetivo** – Padronizar a metodologia de imagem por PET/TC com $^{18}$F-FDG como uma ferramenta de avaliação do modelo experimental de CHC secundário a DHGNA. **Métodos** – Dez ratos Sprague-Dawley machos foram alimentados com dieta hiperlipídica deficiente em colina associada a dietilnitrosamina (DEN) na água de beber por 16 semanas e depois receberam 1 mL de solução salina (0,9%) por gavagem diariamente por três semanas. Nas 16ª e 19ª semanas, foi realizada a ultrassonografia abdominal. As imagens do PET/TC com $^{18}$F-FDG foram obtidas antes do início do experimento (semana 0) e no final (semana 19). Análises histológica e imunohistoquímica também foram realizadas. **Resultados** – Os resultados da ultrassonografia demonstraram um grupo homogêneo na 16ª semana com uma média de 4,6±2,74 nódulos por animal. Na 19ª semana, os achados do PET/CT demonstraram uma média de 8,5±3,7 nódulos por animal. Os valores médios de SUVmed e SUVmáx foram 2,186±0,1698 e 3,8±1,74, respectivamente. A média do número de nódulos na análise histológica foi de 5,5±1,5. De todos os nódulos, 4,6% foram classificados como bem diferenciados e 81,8% foram classificados como CHC pouco diferenciado. **Conclusão** – O PET/TC com $^{18}$F-FDG foi capaz de avaliar o desenvolvimento do CHC secundário a DHGNA de forma não invasiva. A partir da padronização do PET/CT neste modelo, faz-se possível a utilização desta ferramenta em futuros estudos para monitorar, in vivo e de forma não invasiva, a progressão do CHC.

**DESCRITORES** – Carcinoma hepatocelular. Hepatopatia gordurosa não alcoólica. Tomografia computadorizada com tomografia por emissão de pósitrons. Fluordesoxiglucose F18. Modelos animais.

## REFERENCES

1. Vernon G, Baranova A, Younossi ZM. Systematic review: The epidemiology and natural history of non-alcoholic fatty liver disease and non-alcoholic steatohepatitis in adults. Aliment Pharmacol Ther. 2011;34:274-85.
2. Lazo M, Hernaez R, Eberhardt MS, Bonekamp S, Kamel I, Guallar E, et al. Prevalence of nonalcoholic fatty liver disease in the United States: The third national health and nutrition examination survey, 1988-1994. Am J Epidemiol. 2013;178:38-45.
3. Michelotti GA, Machado M V, Diehl AM. NAFLD, NASH and liver cancer. Vol. 10, Nat Rev Gastroenterol Hepatol. 2013;10:656-65.
4. Ferlay J, Soerjomataram I, Dikshit R, Eser S, Mathers C, Rebelo M, et al. Cancer incidence and mortality worldwide: sources, methods and major patterns in GLOBOCAN 2012. Int J cancer. 2015;136:E359-86.
5. Baffy GG, Brunt EM, Caldwell SH. Hepatocellular carcinoma in non-alcoholic fatty liver disease: An emerging menace. J Hepatol. 2012;56:1384-91.
6. Tsatsoulis A, Mantzaris MD, Bellou S, Andrikoula M. Insulin resistance: An adaptive mechanism becomes maladaptive in the current environment - An evolutionary perspective. Metabolism. 2013;62:622-33.

7. Asgharpour A, Cazanave SC, Pacana T, Seneshaw M, Vincent R, Banini BA, et al. A diet-induced animal model of non-alcoholic fatty liver disease and hepatocellular cancer Amon. J Hepatol. 2016;65:579-88.
8. Sanches SCL, Ramalho LNZ, Augusto MJ, Da Silva DM, Ramalho FS. Nonalcoholic Steatohepatitis: A Search for Factual Animal Models. Biomed Res Int. 2015;2015:574832.
9. Yu J, Marsh S, Hu J, Feng W, Wu C. The Pathogenesis of Nonalcoholic Fatty Liver Disease: Interplay between Diet, Gut Microbiota, and Genetic Background. Gastroenterol Res Pract. 2016;2016:2862173.
10. Carvalho CF, Chammas MC, Souza de Oliveira CPM, Cogliati B, Carrilho FJ, Cerri GG. Elastography and Contrast-enhanced Ultrasonography in the Early Detection of Hepatocellular Carcinoma in an Experimental Model of Nonalcoholic Steatohepatitis. J Clin Exp Hepatol. 2013;3:96-101.
11. Hueper K, Elalfy M, Laenger F, Halter R, Rodt T, Galanski M, et al. PET/CT imaging of c-Myc transgenic mice identifies the genotoxic N-nitroso-diethylamine as carcinogen in a short-term cancer bioassay. PLoS One. 2012;7:e30432.
12. Park SI, Lee JH, Ham HJ, Jung YJ, Park MS, Lee J, et al. Evaluation of 2-[18F]-fluoro-2-deoxy-D-glucose positron emission tomography/computed tomography in rat models with hepatocellular carcinoma with liver cirrhosis. Biomed Mater Eng. 2015;26(s1):S1669-76.
13. Park JH, Kang JH, Lee YJ, Kim KI, Lee TS, Kim KM, et al. Evaluation of diethylnitrosamine- or hepatitis B virus X gene-induced hepatocellular carcinoma with 18F-FDG PET/CT: a preclinical study. Oncol Rep. 2015;33:347-53.
14. de Lima VMRVMR, Oliveira CPMSMS, Alves VAFF, Chammas MC, Oliveira EP, Stefano JTJT, et al. A rodent model of NASH with cirrhosis, oval cell proliferation and hepatocellular carcinoma. J Hepatol. 2008;49:1055-61.
15. Kleiner DE, Brunt EM, Van Natta M, Behling C, Contos MJ, Cummings OW, et al. Design and validation of a histological scoring system for nonalcoholic fatty liver disease. Hepatology. 2005;41:1313-21.
16. Thoolen B, Maronpot RR, Harada T, Nyska A, Rousseaux C, Nolte T, et al. Proliferative and nonproliferative lesions of the rat and mouse hepatobiliary system. Toxicol Pathol. 2010;38(7 Suppl.):5-81.
17. Edmondson HA, Steiner PE. Primary carcinoma of the liver: a study of 100 cases among 48,900 necropsies. Cancer. 1954;7:462-503.
18. Hwang GL, van den Bosch MA, Kim YI, Katzenberg R, Willmann JK, Paulmurugan R, et al. Development of a High-Throughput Molecular Imaging-Based Orthotopic Hepatocellular Carcinoma Model. Cureus. 2015;39:324-30.
19. Groß C, Steiger K, Sayyed S, Heid I, Feuchtinger A, Walch A, et al. Model matters: Differences in orthotopic rat hepatocellular carcinoma physiology determine therapy response to sorafenib. Clin Cancer Res. 2015;21:4440-50.
20. Lee J-S, Chu I-S, Mikaelyan A, Calvisi DF, Heo J, Reddy JK, et al. Application of comparative functional genomics to identify best-fit mouse models to study human cancer. Nat Genet. 2004;36:1306-11.
21. Dowman JK, Hopkins LJ, Reynolds GM, Nikolaou N, Armstrong MJ, Shaw JC, et al. Development of hepatocellular carcinoma in a murine model of nonalcoholic steatohepatitis induced by use of a high-fat/fructose diet and sedentary lifestyle. Am J Pathol. 2014;184:1550-61.
22. Ikawa-Yoshida A, Matsuo S, Kato A, Ohmori Y, Higashida A, Kaneko E, et al. Hepatocellular carcinoma in a mouse model fed a choline-deficient, L-amino acid-defined, high-fat diet. Int J Exp Pathol. 2017;98:221-33.
23. Yamamoto Y, Nishiyama Y, Kameyama R, Okano K, Kashiwagi H, Deguchi A, et al. Detection of hepatocellular carcinoma using 11C-choline PET: comparison with 18F-FDG PET. J Nucl Med. 2008;49:1245-8.
24. Trojan J, Schroeder O, Raedle J, Baum RP, Herrmann G, Jacobi V, et al. Fluorine-18 FDG positron emission tomography for imaging of hepatocellular carcinoma. Am J Gastroenterol. 1999;94:3314-9.
25. Kornberg A, Schernhammer M, Friess H. 18F-FDG-PET for Assessing Biological Viability and Prognosis in Liver Transplant Patients with Hepatocellular Carcinoma. J Clin Transl Hepatol. 2017;5:224-34.
26. Sugiyama M, Sakahara H, Torizuka T, Kanno T, Nakamura F, Futatsubashi M, et al. 18F-FDG PET in the detection of extrahepatic metastases from hepatocellular carcinoma. J Gastroenterol. 2004;39:961-8.
27. Park J-W, Kim JH, Kim SK, Kang KW, Park KW, Choi J-I, et al. A prospective evaluation of 18F-FDG and 11C-acetate PET/CT for detection of primary and metastatic hepatocellular carcinoma. J Nucl Med. 2008;49:1912-21.
28. Yoon KT, Kim JK, Kim DY, Ahn SH, Lee JD, Yun M, et al. Role of 18F-fluorodeoxyglucose positron emission tomography in detecting extrahepatic metastasis in pretreatment staging of hepatocellular carcinoma. Oncology. 2007;72 Suppl 1:104-10.
29. Kinkel K, Lu Y, Both M, Warren RS, Thoeni RF. Detection of hepatic metastases from cancers of the gastrointestinal tract by using noninvasive imaging methods (US, CT, MR imaging, PET): a meta-analysis. Radiology. 2002;224:748-56.
30. Lin CY, Chen JH, Liang JA, Lin CC, Jeng L Bin, Kao CH. 18F-FDG PET or PET/CT for detecting extrahepatic metastases or recurrent hepatocellular carcinoma: A systematic review and meta-analysis. Eur J Radiol. 2012;81:2417-22.
31. Tsurusaki M, Okada M, Kuroda H, Matsuki M, Ishii K, Murakami T. Clinical application of 18F-fluorodeoxyglucose positron emission tomography for assessment and evaluation after therapy for malignant hepatic tumor. J Gastroenterol. 2014;49:46-56.
32. Torizuka T, Tamaki N, Inokuma T, Magata Y, Yonekura Y, Tanaka A, et al. Value of fluorine-18-FDG-PET to monitor hepatocellular carcinoma after interventional therapy. J Nucl Med. 1994;35:1965-9.
33. Cascales-Campos PA, Ramirez P, Lopez V, Gonzalez R, Saenz-Mateos L, Llacer E, et al. Prognostic Value of 18-Fluorodeoxyglucose-Positron Emission Tomography After Transarterial Chemoembolization in Patients With Hepatocellular Carcinoma Undergoing Orthotopic Liver Transplantation. Transplant Proc. 2015;47:2374-6.
34. Kornberg A, Witt U, Matevossian E, Kupper B, Assfalg V, Drzezga A, et al. Extended postinterventional tumor necrosis-implication for outcome in liver transplant patients with advanced HCC. PLoS One. 2013;8:e53960.
35. Siemerink EJM, Mulder NH, Brouwers AH, Hospers GAP. 18F-Fluorodeoxyglucose positron emission tomography for monitoring response to sorafenib treatment in patients with hepatocellular carcinoma. Oncologist. 2008;13:734-7.
36. Lee JDJH, Park JY, Kim DY, Ahn SH, Han K-HH, Seo HJ, et al. Prognostic value of 18F-FDG PET for hepatocellular carcinoma patients treated with sorafenib. Liver Int. 2011;31:1144-9.
37. Seo S, Hatano E, Higashi T, Hara T, Tada M, Tamaki N, et al. Fluorine-18 fluorodeoxyglucose positron emission tomography predicts tumor differentiation, P-glycoprotein expression, and outcome after resection in hepatocellular carcinoma. Clin Cancer Res. 2007;13:427-33.
38. Sun D-W, An L, Wei F, Mu L, Shi X-J, Wang C-L, et al. Prognostic significance of parameters from pretreatment (18)F-FDG PET in hepatocellular carcinoma: a meta-analysis. Abdom Radiol (New York). 2016;41:33-41.
39. Detry O, Govaerts L, Deroover A, Vandermeulen M, Meurisse N, Malenga S, et al. Prognostic value of 18F-FDG PET/CT in liver transplantation for hepatocarcinoma. World J Gastroenterol. 2015;21(10):3049-54.
40. Lee SD, Kim S-KSH, Kim Y-K, Kim C, Kim S-KSH, Han S-S, et al. 18 F-FDG-PET/CT predicts early tumor recurrence in living donor liver transplantation for hepatocellular carcinoma. Transpl Int. 2013;26:50-60.
41. Lee SD, Lee B, Kim S-KSH, Joo J, Kim S-KSH, Kim Y-K, et al. Proposal of new expanded selection criteria using total tumor size and 18 F-fluorodeoxyglucose - positron emission tomography/computed tomography for living donor liver transplantation in patients with hepatocellular carcinoma: The National Can. World J Transplant. 2016;6:411.